Vol. 18, pp. 274–283 (2021)
doi: 10.2142/biophysico.bppb-v18.033

Biophysics and Physicobiology
https://www.jstage.jst.go.jp/browse/biophysico/

Review Article (Invited)

The insights into calcium ion selectivity provided by ancestral prokaryotic ion channels

Katsumasa Irie[1,2]

[1] *Department of Biophysical Chemistry, School of Pharmaceutical Sciences, Wakayama Medical University, Wakayama 640-8156, Japan*
[2] *Cellular and Structural Physiology Institute (CeSPI), Nagoya University, Nagoya, Aichi 464-8601, Japan*

Received October 4, 2021; Accepted November 16, 2021;
Released online in J-STAGE as advance publication November 19, 2021
Edited by Shigetoshi Oiki

Prokaryotic channels play an important role in the structural biology of ion channels. At the end of the 20th century, the first structure of a prokaryotic ion channel was revealed. Subsequently, the reporting of structures of various prokaryotic ion channels have provided fundamental insights into the structure of ion channels of higher organisms. Voltage-dependent Ca^{2+} channels (Cavs) are indispensable for coupling action potentials with Ca^{2+} signaling. Similar to other proteins, Cavs were predicted to have a prokaryotic counterpart; however, it has taken more than 20 years for one to be identified. The homotetrameric channel obtained from *Meiothermus ruber* generates the calcium ion specific current, so it is named as CavMr. Its selectivity filter contains a smaller number of negatively charged residues than mutant Cavs generated from other prokaryotic channels. CavMr belonged to a different cluster of phylogenetic trees than canonical prokaryotic cation channels. The glycine residue of the CavMr selectivity filter is a determinant for calcium selectivity. This glycine residue is conserved among eukaryotic Cavs, suggesting that there is a universal mechanism for calcium selectivity. A family of homotetrameric channels has also been identified from eukaryotic unicellular algae, and the investigation of these channels can help to understand the mechanism for ion selection that is conserved from prokaryotes to eukaryotes.

Key words: electrophysiology, structural biology, ion permeation, protein evolution

Significance

Prokaryotic proteins play an important role in the structural biology. Voltage-dependent Ca^{2+} channels (Cavs) are indispensable for coupling action potentials with Ca^{2+} signaling. Cavs were also predicted to have a prokaryotic counterpart; however, it has not been identified, yet. The homotetrameric channel obtained from *Meiothermus ruber* generates the calcium ion specific current. This channel belongs to a different cluster of phylogenetic trees than canonical prokaryotic channels. The glycine residue of its selectivity filter is a determinant for Ca^{2+} selectivity. This glycine residue is well conserved among eukaryotic Cavs, suggesting that there is a universal mechanism for Ca^{2+} selectivity.

Introduction

The control of thinking, memory formation, and muscle contraction is attributed to neural activity. The transmission of electrical stimulation occurs through various cation-selective channels on the neural cell membrane [1]. For example, the influx of sodium ion (Na^+) by voltage-dependent sodium channels (Navs) transmits action potentials, and the outflow of

Corresponding author: Katsumasa Irie, Department of Biophysical Chemistry, School of Pharmaceutical Sciences, Wakayama Medical University, 25-1, Shichibancho, Wakayama, 640-8156, Japan. ORCID iD: https://orcid.org/0000-0002-8178-1552, e-mail: kirie@wakayama-med.ac.jp

potassium ion (K^+) by voltage-dependent potassium channels (Kvs) rapidly renders the membrane potential to resting potential. Subsequently, the action potential reaches the presynapse, and activates the voltage-dependent calcium channels (Cavs) to cause the influx of calcium ion (Ca^{2+}) into the cell. Through a series of intracellular signals from the influx of Ca^{2+}, neurotransmitters are released into the synaptic cleft, causing the activation of ionotropic receptors, which generate action potentials. These steps comprise the transition process of the neural stimulus to the next nerve cell. Thus, the selective permeation of cations is essential for the accurate transmission of neural transduction.

Prokaryotic ion channels have played a major role in elucidating the molecular mechanism of ion selectivity. The structure of KcsA, which is first atomic resolution structure of ion channels, has provided detailed mechanisms for the selective permeation of K^+ and gating (Fig. 1a) [2–4]. Even today, KcsA is actively used in advanced research and methods in computational science and biophysical chemistry because of its simplicity and robustness [5–7]. KcsA is homotetrameric channel, and the monomer of KcsA contains two transmembrane helices and forms tetrameric pore domain. The selectivity filter (SF), which plays important role for ion selectivity, locates between two transmembrane helices of the monomer and forms the ion permeation pore at the center of pore domain (Fig. 1a). The basic structure of the pore domain is conserved in many cation channels, including ligand-activated ionotropic receptor-type channels, some of which have opposite insertion directions into the lipid membrane [8,9]. Similarly, many prokaryotic sodium channels (BacNavs) have been characterized [10–12] and provide various insights into sodium selectivity and channel mechanism (Fig. 1b) [13–15]. BacNavs are homotetrameric channels, which have additional four helices at N-terminal of two helices of pore domain (Fig. 1b left). The N-terminal four helices of each monomer individually form the voltage sensing domain. Therefore, four voltage sensing domains are located around the pore domain (Fig. 1b right). This structure is also shared by Kv and TRP channels, which are temperature-sensitive channels [16,17]. In contrast, natural prokaryotic Cavs remained undiscovered for nearly 20 years after the discovery of the first bacterial channel, despite the prediction of their existence since the discovery of these bacterial ion channels. Instead of finding a native prokaryotic Cav, the mutation to gain calcium selectivity has been found on BacNavs [18,19]. These Ca^{2+} selective BacNav mutants have been subjected to extensive studies. However, these Ca^{2+} selective mutations have

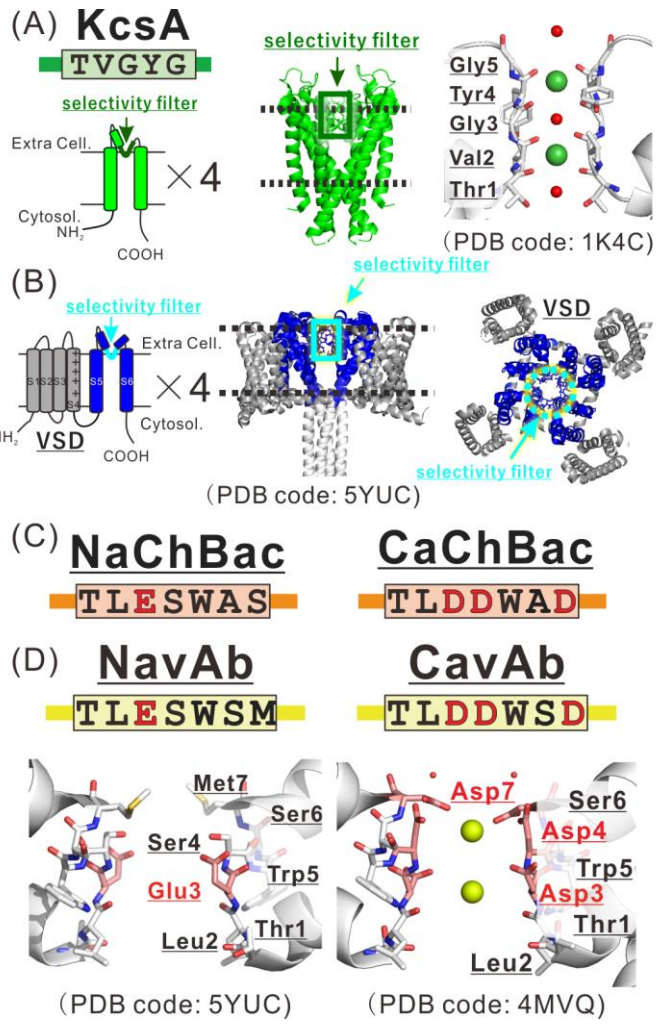

Figure 1 Schematic secondary structure and 3D structure of tetrameric cation channels.
(A). Left: Schematic secondary structure of KcsA. Extra cell. indicates extra-cellular side, and Cytosol. indicates cytosolic side. The cylinder indicates the α-helix. The pore domain of KcsA is colored green. Center: 3D structure of KcsA from horizontal viewing to lipid bilayer [PDB ID: 1K4C]. Right: Detail structure of the SF of KcsA. The green and red balls indicate potassium ions and water molecule, respectively. (B). Left: Schematic secondary structure of BacNav. The pore domain of BacNav is colored blue, The voltage sensing domain (VSD) is colored gray. Center: 3D structure of BacNav with horizontal viewing to lipid bilayer [PDB ID: 5YUC]. Right: 3D structure of BacNav with vertical viewing from extracellular side. (C). The SF sequence of NaChBac and CaChBac. The SF sequences are indicated using single letter codes. Negatively charged residues are colored in red. (D). The SF sequence and 3D structure of NavAb [PDB ID: 5YUC] and CavAb [PDB ID: 4MVQ]. Negatively charged residues are colored in red. The carbon atoms of negatively charged residues were indicated in pink. The yellow balls indicate calcium ions.

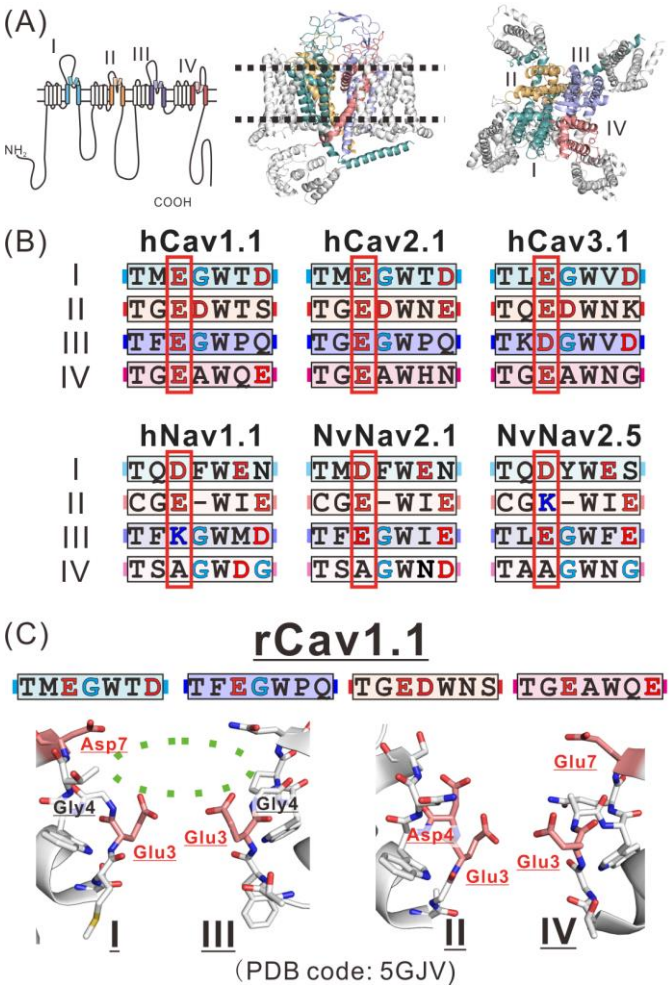

Figure 2 3D structure and SF sequence of 24TM Cav. (A). Left: Schematic secondary structure of 24TM Cav pore domain. The cylinder indicates the α-helix. The pore domain of subdomains I, II, III, and IV of Cav are colored green, yellow, purple, and red, respectively. Center: 3D structure of rabbit Cav1.1 with horizontal viewing to lipid bilayer [PDB ID: 5GJV]. Right: 3D structure of rabbit Cav1.1 with vertical viewing from extracellular side. (B). SF sequence of 24TM channels. The SF sequences are indicated using single letter codes. Negatively charged residues are colored in red. Glycine residues in the position 4 are colored in cyan. The straight lines indicate the luck residue. The selectivity filter sequence of human Cav1.1 (hCav1.1) (UniProt ID: Q13698), hCav2.1 (O00555), hCav3.1 (O43497), hNav1.1 (P35498), *Nematostella vectensis* Nav2.1 (NvNav2.1) (I6NKP7) and NvNav2.5 (I6NQG1), were indicated. (C). SF sequence and SF structure of rabbit Cav1.1 (rCav1.1). The subdomains I and III (left), and II and IV (right) are shown separately. The carbon atoms of negatively charged residues were indicated in pink. The dashed green circle indicates the wide entrance of the SF.

not been found in native channels. Therefore, finding putative Cav supposed to exist in prokaryotes will help us to understand the evolutional development of calcium selectivity mechanisms.

Selectivity filter of tetrameric channels

The SF sequence of KcsA is constructed by five residues "TVGYG" (Fig. 1a), while that of BacNav is constructed by seven residues, added two residues at the C-terminal side. The SF sequences of NaChBac, which is firstly cloned BacNav [10], and NavAb, which is firstly structure-determined homologue of BacNav [13], are "TLESWAS" and "TLESWSM" (Fig. 1c, d left). Although the SF of K channel has no charged residue (Fig. 1a right), BacNavs contain one charged residue at the position 3 (Fig. 1c, d left). Glu3 of BacNavs SF is important for ion permeation. Four glutamate residues are densely located in a narrow pathway of the ion permeation pore (Fig. 1d left). Therefore, some of the four glutamates are considered to be protonated. The molecular dynamics simulations of BacNavs predicted that the sodium ions efficiently permeate the ion pore when one of the four glutamates of SF is protonated [20]. It means that even if subunits are homotetrameric, the protonation states of the SFs would be heterotetrameric. The Ca^{2+} selective BacNav mutants are obtained by the introduction of the negatively charged amino acid into the SF (Fig. 1d right) [18,19]. The calcium-selective mutants of NaChBac and NavAb are named as CaChBac and CavAb, whose SF sequences are "TLDDWAD" and "TLDDWSD", respectively (Fig. 1c, d right) [18,19]. The protonation state of CaChBac and CavAb SF would be also asymmetric as well, and more complicated than sodium channels' one.

As if in support of the idea that charge-hetero selective filters are effective in selective permeation of sodium and calcium, the ion-permeation pore of Cav and Navs is asymmetric in higher organisms (Fig. 2a). Mammalian Nav and Cav contain 24 transmembrane helices (24TM) characterized by four homologous repeats, which each contains six-transmembrane helices corresponding to tetrameric channel monomer (Fig. 2a) [21]. Of course, these SF sequences are also asymmetric (Fig. 2b). Considering their homology, it has been proposed that Cavs and Navs have the same evolutionary origin [22]. Their two pairs of subdomains, subdomain I and III, and subdomain II and IV, are evolutionarily close to each other, respectively [23,24]. 24TM Navs and Cavs would be generated by two times of gene duplication of same homotetrameric channels or gene fusion of other homotetrameric channels in the process of evolution. After then, each repeat becomes a homologous subdomain. The SF sequences among the subdomains of 24TM Nav is more diverse than that of 24TM Cav (Fig. 2b). Invertebrates have a channel similar to mammalian Nav, called Nav2 (Fig. 2b) [22]. This channel group is

located between human Cav and Nav in the phylogenetic tree. These suggest that 24TM Cav is closer to the root on the evolutionary tree than 24TM Nav. In the case of 24TM channels, Cavs have more negatively charged residues than Nav, which gave the idea for the mutation that gives BacNavs calcium selectivity.

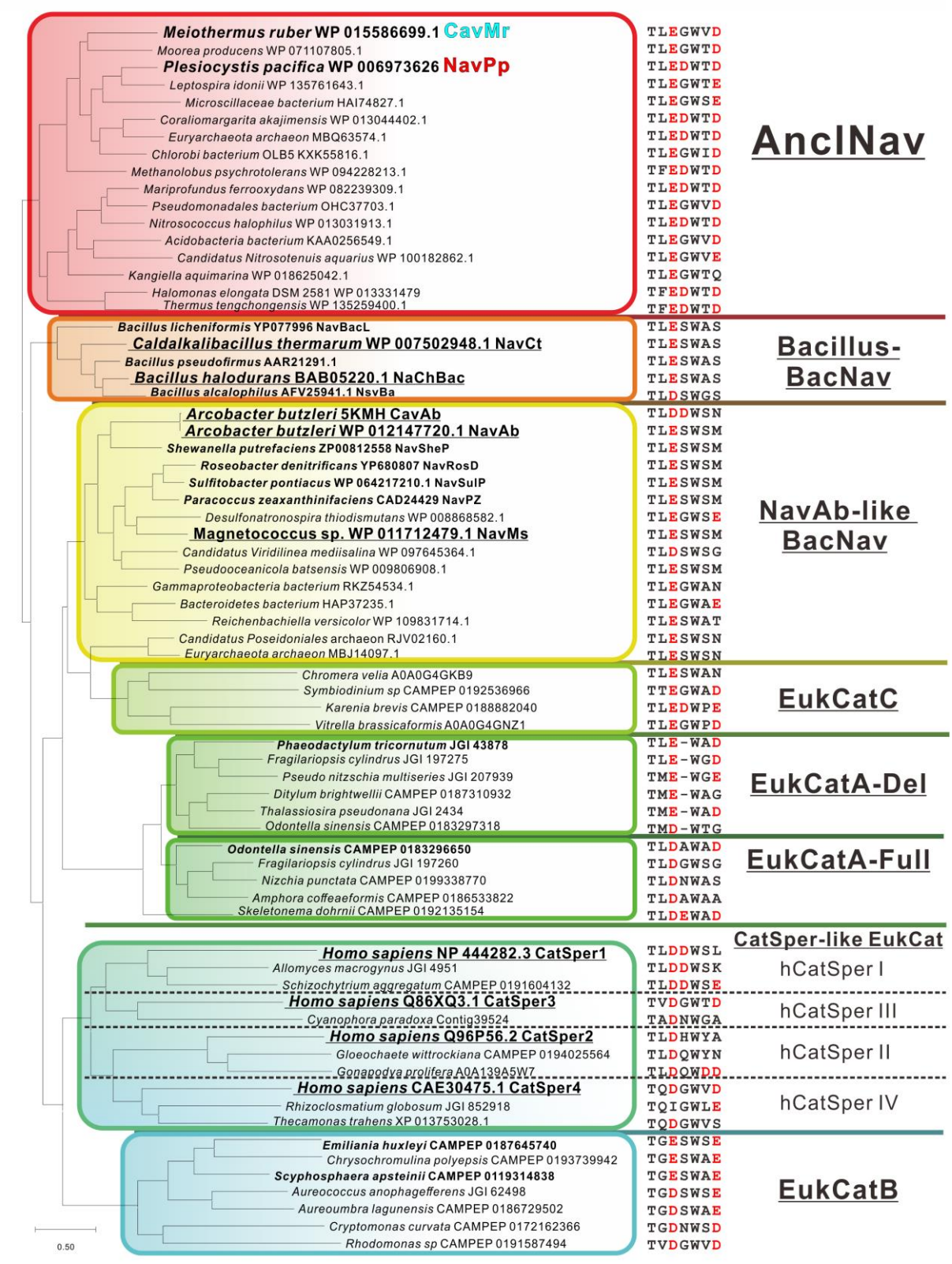

Figure 3 Sequence analysis shows that AnclNavs form a novel class of homotetrameric cation channels.
Phylogenetic tree of the homotetrameric channels. The MEGA7 program was used to align the multiple protein sequences of the BacNav homologs and generate the phylogenetic tree. EukCats and representatives of the specialized family of heterotetrameric channel identified in mammalian sperm (CatSpers) were also included, based on a previous study [36]. EukCatA sequences were divided into two groups, EukCatA-Del and EukCatA-Full, based on the deletion of the fourth residue of the SF. The branch lengths are proportional to the sequence divergence, with the scale bar corresponding to 0.1 substitutions per amino acid position. SF for each sequence is shown (right). First threonine residue is assigned as "Position 1." Negatively charged residues are colored red.

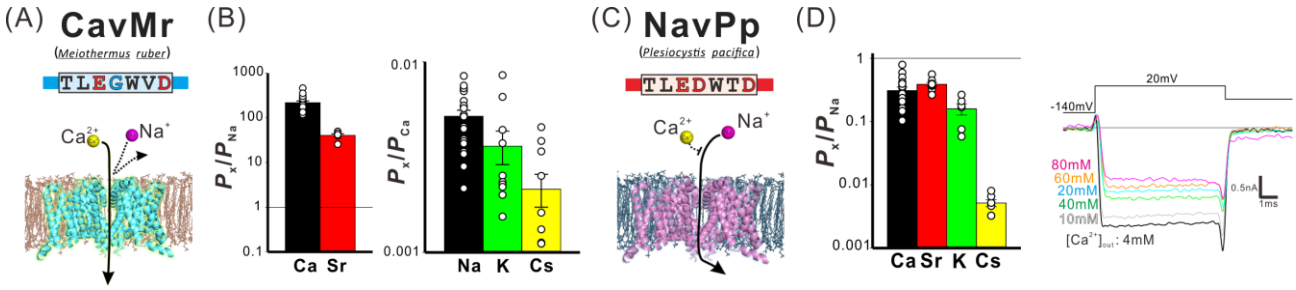

Figure 4 The cation selectivity of CavMr and NavPp.
(A). Homology model and SF sequence of CavMr. Schematic representation of ion selectivity using a homology model based on NavAb structure [PDB ID: 5YUC]. The SF sequences are indicated using single letter codes. Negatively charged residues are colored in red. Glycine residues in the fourth position are colored in cyan. (B). The relative permeability of Ca^{2+} or Sr^{2+} to Na^{+} and each monovalent cation to Ca^{2+} in CavMr. (C). Homology model and SF sequence of NavPp. Schematic representation of ion selectivity using a homology model based on NavAb structure [PDB ID: 5YUC]. The SF sequences are indicated using single letter codes. Negatively charged residues are colored in red. (D). Left: The relative permeability of Ca^{2+}, Sr^{2+}, K^{+}, and Cs^{+} to Na^{+} in NavPp. Right: Representative current traces of NavPp generated by +20 mV stimulation pulses in solutions with various concentrations of extracellular Ca^{2+}.

Discovery of new groups of homotetrameric channels

The three-dimensional structure of CavAb indicated that the negatively charged SF traps divalent cation such as Ca^{2+} more than mono valent cation such as Na^{+}, which nicely explains the selective permeation mechanism of Ca^{2+} [18]. However, there is no native Ca^{2+}-selective channel with CavAb or CaChBac SF sequence. Moreover, there is a large difference in the number of negatively charged residues in the SFs between artificial BacCavs (CaChBac and CavAb) and 24TM Cav. The number of negatively charged residues of CaChBac and CavAb SF is 12 (Fig. 1c, d), and that of 24TM Cav is 7 (Fig. 3b, c). The charged environment in each pore must be very different depending on this charge difference (Fig. 1d, 2c). On the other hand, even though there are differences in the amount of charge in prokaryotic and eukaryotic channels, it is true that calcium selectivity is increased by the introduction of negative charge into the SF [18,19]. There is a prediction that the SF of the ancestral BacNav has increased negative charge [25], and native BacCav had been unidentified. Therefore, the identification of the native BacCav would be an important insight into the evolution of cation channels and the universal calcium selectivity. The new homotetrameric channel group, identified as **Anc**estor-**l**ike Bac**Nav** (AnclNav), have CavMr, the first prokaryotic Cav (Fig. 3) [26], and will live up to these expectations.

Based on the prediction that the ancestral channels have more negative charges in the SF than the BacNav channel [25], AnclNav was discovered [26]. The SF sequences of AnclNav is similar to that of the predicted ancestral BacNav, and have one or two more negatively charged residues than canonical BacNavs, which were in a Bacillus group and a NavAb-like group (Fig. 3) [26]. Although AnclNavs keep overall homology with the canonical BacNavs, they apparently belong to a different branch of the phylogenetic tree each other (Fig. 3). AnclNav genes were also found in bacteria of the phylum *Deinococcus-Thermus*, which is closer to the last universal common ancestor than the existing BacNav host [27].

Identification of prokaryotic Ca channel and comparison of the ion permeation mechanism

It is known that BacNavs are transiently well expressed in insect cells and generate a large current by plasmid transfection [28]. With the same method, whole-cell patch-clamp experiments in insect cells confirmed the presence of

ion channel currents of the AnclNav gene isolated from *Meiothermus ruber* and *Plesiocystis pacifica* (Fig. 4). In particular, the channel derived from *M. ruber* showed high Ca^{2+} permeability (Fig. 4a, b). This channel is the first prokaryotic Cav discovered in the world, and was named CavMr from the species name. CavMr had a P_{Ca}/P_{Na} of 218 ± 38 [26]. This high P_{Ca}/P_{Na} value was comparable with that of CavAb[18]. CavMr did not allow Na^+ permeation under Ca^{2+}-free conditions [26]. CavMr does not require a small amount of Ca^{2+} for calcium selectivity, as has been observed with mammalian Cavs [29]. The SF of CavMr contains a glycine residue at position 4 and a negatively charged residue at position 7 (Fig. 4a), which were not observed in the canonical BacNav family.

The other AnclNav from *P. pacifica* (NavPp) easily permeates Na^+, but its current was blocked by Ca^{2+} (Fig. 4c, d). This feature was also not found in the canonical BacNavs. Interestingly, the SF of NavPp has one more aspartate residue than that of CavMr and a similar number to those of the artificial Ca^{2+}-selective BacNav mutants, CaChBac and CavAb [18, 19]; however, NavPp does not show calcium selectivity. The mutants, NavPp-T6A and NavPp-T6S, have same SF sequence as CaChBac and CavAb, respectively (Fig. 4) [18, 19]. However, each channel exhibited Ca^{2+}-blocked currents, similar to wild-type NavPp [26]. Therefore, both of the SF sequences providing calcium selectivity to canonical BacNavs failed to generate Ca^{2+}-permeable NavPp. Conversely, CavMr-D7M, a mutant that reduces the number of acidic amino acids in the SF, maintained high calcium selectivity [26]. These results were inconsistent with the conventional model based on the artificial Cav, CaChBac and CavAb. Furthermore, the mutants of NavPp and CavMr in which the selective filters were replaced with that of NavAb did not show channel activity [26]. The difference in ion selectivity between AnclNav and canonical BacNav, even after mutated to the same filter sequence, suggested that there were differences in the pore domain structure between AnclNav and canonical BacNav.

Commonality of ion permeation mechanisms among AnclNavs

NavPp-Mr, in which the SF is replaced with that of CavMr, has a reduced number of acidic amino acids, but attained high calcium selectivity (Fig. 5a) [26]. In contrast, CavMr-Pp, which is a mutant containing more acidic amino acids, became a non-selective cation channel and its calcium selectivity was significantly impaired (Fig. 5b) [26].

The residues of positions 4 and 6 of CavMr and NavPp were different, so that alternate single mutations of these residues create the same SF sequence. CavMr-V6T and NavPp-D4G have the same SF sequence ("TLEGWTD") and showed high calcium selectivity over Na^+ (Fig. 5c) [26]. CavMr-G4D and NavPp-T6V, with the SF sequence "TLEDWVD", failed to attain calcium selectivity but allowed K^+ and Cs^+ permeation (Fig. 5d) [26]. This SF is unprecedented in that it has the highest selectivity for Sr^{2+}. Interestingly, CavMr and NavPp mutants with the same selective filter sequences showed similar ion permeability. In the cases of CavMr and NavPp, a glycine residue at position 4 is a key determinant of calcium selectivity and a valine residue at position 6 has a supportive effect on divalent cation selectivity. It can be considered that there is a correlation between the filter sequence and the ion selectivity of AnclNavs, and that they share a similar channel structure.

Comparison of the selectivity filter sequence of three Ca-selective channels

The comparison of the amino acid sequences of the SFs of the three Ca^{2+}-selective channels, namely CavMr and CavAb and the human Cav, revealed several characteristic features. The charged residues of CavMr SF were similar to those of

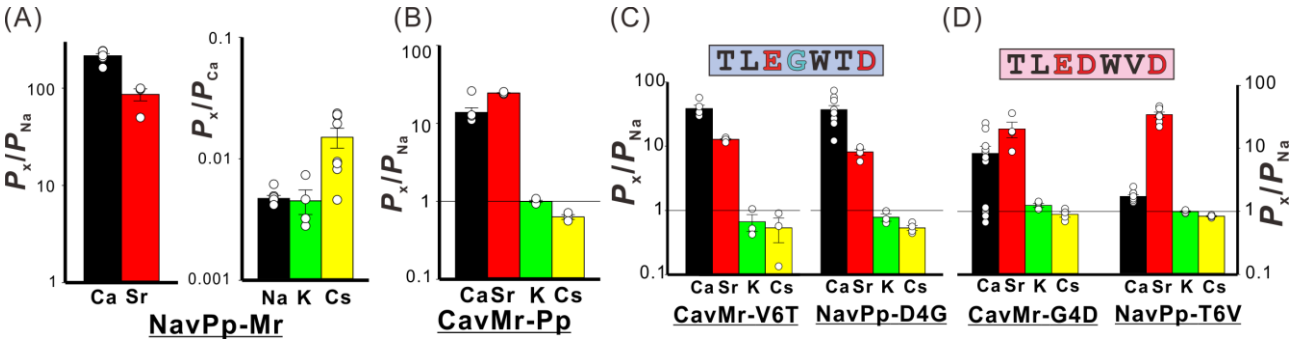

Figure 5 The cation selectivity of CavMr and NavPp mutants.
(A) The relative permeability of divalent cations to Na^+ (left) and that of monovalent cations to Ca^{2+} (right) in NavPp-Mr. (B) The relative permeability of different cations to Na^+ in CavMr-Pp. (C) The relative permeability of each cation to Na^+ in the SF sequence "TLEGWTD" mutants derived from CavMr and NavPp. (D) The relative permeability of each cation to Na^+ in the SF sequence "TLEDWVD" mutants derived from CavMr and NavPp.

human Cav subdomains. The selective filters of both human Cav and CavMr have fewer acidic amino acid residues than that of CavAb (Fig. 1d and 2c).

The selectivity of several mutants indicated that the fourth glycine residue is more important than the acidic amino acid, aspartic acid, for the calcium selectivity of AnclNav type. This fourth glycine residue is also well conserved in subdomains I and III of mammalian Cav. That of Cav3.1 is even the same as that of CavMr (Fig. 2b, 4a), but the 4th glycine residue has not been studied for selectivity in previous studies. CavMr highlights the importance of previously overlooked glycine residues, and reminds us of the existence of a highly conserved calcium selectivity mechanism from prokaryotes to eukaryotes.

Although the three-dimensional structure of CavMr has not been available, the structure of rabbit Cav1.1 subdomain I and III provides the similar SF structure of CavMr (Fig. 2c left) [30]. It can be seen that the extracellular entrance of the selective filter has a wider space than CavAb by facing the subdomains I and III with the 4th glycine residue (Fig. 2c left: green frame). It can be assumed that the existence of this space contributes to the improvement in calcium selectivity.

CavAb is a mutant of NavAb and its structure is most analyzed among the Ca^{2+}-selective channels [18]. Although the three-dimensional structures of CavAb exactly provide one of the structural bases of calcium selectivity, the importance of the glycine residue for calcium selectivity could not be determined from the structure of CavAb. The SF sequences of CavAb and CaChBac were more similar to those of 24TM Cav subdomains II and IV than I and III (Fig. 1d, 2c and 4b). NavPp has similar SF sequence to CavAb. It may be that channels with CavMr or CavAb/NavPp-like SFs each provided a partial mechanism of calcium selectivity to 24TM-type channels in the ancient times. In other words, 24TM Cav looks like a hybrid channel of CavMr and NavPp.

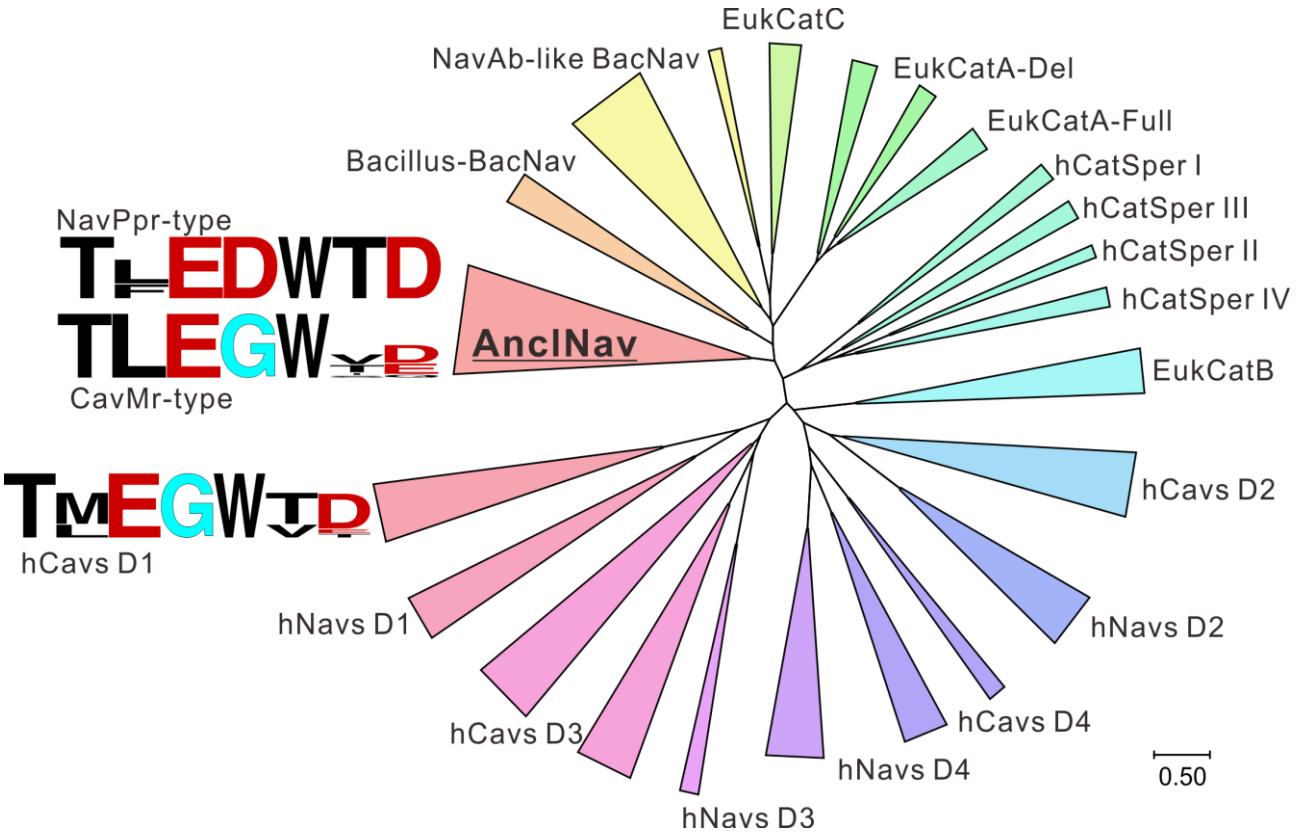

Figure 6 Abbreviated phylogenetic tree of tetrameric cation channels with each subdomain of human 24TM voltage-gated cation channels.

Protein sequences of human Cavs (Cav1.1, Cav1.2, Cav1.3, Cav1.4, Cav2.1, Cav2.2, Cav2.3, Cav3.1, Cav3.2, and Cav3.3) and Navs (Nav1.1, Nav1.2, Nav1.3, Nav1.4, Nav1.5, Nav1.6, Nav1.7, Nav1.8, and Nav1.9) were divided into four subdomains and phylogenetically analyzed (D1–D4) with other single domain type of channels used in Figure 2. For visibility, each cluster is represented as a single triangle. The branch lengths are proportional to the sequence divergence, with the scale bar corresponding to 0.5 substitutions per amino acid position.

Keystones to tracing the evolution of tetrameric cation channels

The discovery of CavMr demonstrates the existence of prokaryotic Cav that has been expected to exist but has not been discovered for a long time. The AnclNav group to which CavMr belongs is likely to be a channel that retains the characteristics of the ancestral and universal mechanism. As shown by CavMr, the fourth glycine residue of the SF is exactly the universal keystone for calcium selectivity. This glycine residue is widely shared from CavMr to human Cav, despite their distance on the phylogenetic tree (Fig. 6). It is thought that there is an important mechanism for calcium selectivity conserved during the evolution from prokaryotes to eukaryotes. Therefore, the structure of CavMr can provide important insights into the molecular mechanism of calcium selectivity.

And then, NavPp is a similarly interesting channel, in which the current is blocked by Ca^{2+}. Divalent cation blocking is observed in various of cation channels [8]. One of a characteristic phenomenon is observed in the ligand-activated channel, NMDA receptor [31]. The current through the NMDA receptor is blocked by Mg ions in a voltage-dependent manner. Although the atomic structures of these channels have been elucidated in recent years [32,33], the molecular mechanism of divalent cation blocking has not yet been elucidated. The divergence of the ligand-activated channels from the voltage-dependent channel is expected to have occurred at an even earlier stage than the acquisition of ion selectivity. Therefore, it is interesting that NavPp, a homolog of AnclNav, showed divalent cation blocking, similar to ancient divergent species, ligand-activated channels. For NMDA receptors, functional analysis experiments and simulations suggested that the SF residues of NMDA receptors were involved in magnesium inhibition [34]. Whether these mechanisms are identical will require further analysis, NavPp, which has a simpler structure, will be a powerful tool for elucidating the divalent cation blocking mechanism.

In recent years, another homotetrameric channel group has been identified in unicellular eukaryotes such as diatoms; this group has been named EukCat (Fig. 3) [35]. The EukCat group also contains Na^+-selective channels [36]. Interestingly, some EukCat homologs have homology to each subunit of CatSper, a eukaryotic heterotetrameric ion channel [37]. EukCat could be the ancestral eukaryotic channel from which the 24TM channel is generated. In this group, a homolog has also been found that lacks the fourth residue of the SF (Fig. 3: EukCatA-Del), which is a characteristic feature found in the subdomain II of 24TM type Navs (Fig. 2b) [38]. Therefore, prokaryotic AnclNavs and the eukaryotic EukCats, as well as BacNavs, are keystones for the elucidation of the ion channel evolution, and the function of them will provide clues as to the establishment of the ion selectivity, which are basic elements of our thinking and memory formation.

Conflict of Interest

The authors declare no competing financial interests.

Author Contributions

K. I. wrote the manuscript.

Acknowledgments

I appreciate Dr. Yoshinori Fujiyoshi for his continuous support in conducting experiments during all of my times in Fujiyoshi labs. I thank Dr. Takushi Shimomura for his works and discussions about ion channels. This work was supported by Grants-in-Aid for Scientific Research (17K17795 and 20K09193), SEI Group CSR Foundation, and Institute for Fermentation, Osaka. The author would like to thank Enago (www.enago.jp) for the English language review.

References

[1] Hille, B. Ion Channels of Excitable Membranes, Third Edtition (Sunderland, MA). (2001).
[2] Doyle, D. A., Cabral, J. M., Pfuetzner, R. A., Kuo, A., Gulbis, J. M., Cohen, S. L., et al. The structure of the potassium channel: Molecular basis of K^+ conduction and selectivity. Science 280, 69–77 (1998). https://doi.org/10.1126/science.280.5360.69
[3] Cuello, L. G., Jogini, V., Cortes, D. M., Perozo, E. Structural mechanism of C-type inactivation in K^+ channels. Nature 466, 203–208 (2010). https://doi.org/10.1038/nature09153
[4] Jiang, Y., Lee, A., Chen, J., Cadene, M., Chait, B. T., MacKinnon, R. The open pore conformation of potassium channels. Nature 417, 523–526 (2002). https://doi.org/10.1038/417523a
[5] Sumino, A., Sumikama, T., Uchihashi, T., Oiki, S. High-speed AFM reveals accelerated binding of agitoxin-2 to a K^+ channel by induced fit. Sci. Adv. 5, eaax0495 (2019). https://doi.org/10.1126/sciadv.aax0495

[6] Sumikama, T., Oiki, S. Digitalized K^+ Occupancy in the Nanocavity Holds and Releases Queues of K^+ in a Channel. J. Am. Chem. Soc. 138, 10284–10292 (2016). https://doi.org/10.1021/jacs.6b05270
[7] Mita, K., Sumikama, T., Iwamoto, M., Matsuki, Y., Shigemi, K., Oiki, S. Conductance selectivity of Na^+ across the K^+ channel via Na^+ trapped in a tortuous trajectory. Proc. Natl. Acad. Sci. U.S.A. 118, e2017168118 (2021). https://doi.org/10.1073/pnas.2017168118
[8] Hamada, K., Mikoshiba, K. IP_3 Receptor Plasticity Underlying Diverse Functions. Annu. Rev. Physiol. 82, 151–176 (2020). https://doi.org/10.1146/annurev-physiol-021119-034433
[9] Chen, S., Gouaux, E. Structure and mechanism of AMPA receptor - auxiliary protein complexes. Curr. Opin. Struct. Biol. 54, 104–111 (2019). https://doi.org/10.1016/j.sbi.2019.01.011
[10] Ren, D., Navarro, B., Xu, H., Yue, L., Shi, Q., Clapham, D. E. A prokaryotic voltage-gated sodium channel. Science 294, 2372–2375 (2001). https://doi.org/10.1126/science.1065635
[11] Irie, K., Kitagawa, K., Nagura, H., Imai, T., Shimomura, T., Fujiyoshi, Y. Comparative study of the gating motif and C-type inactivation in prokaryotic voltage-gated sodium channels. J. Biol. Chem. 285, 3685–3694 (2010). https://doi.org/10.1074/jbc.m109.057455
[12] Koishi, R., Xu, H., Ren, D., Navarro, B. A superfamily of voltage-gated sodium channels in bacteria. J. Biol. Chem. 279, 9532–9538 (2004). https://doi.org/10.1074/jbc.M313100200
[13] Payandeh, J., Gamal El-Din, T. M., Scheuer, T., Zheng, N., Catterall, W. A. Crystal structure of a voltage-gated sodium channel in two potentially inactivated states. Nature 486, 135–139 (2012). https://doi.org/10.1038/nature11077
[14] Tsai, C. J., Tani, K., Irie, K., Hiroaki, Y., Shimomura, T., McMillan, D. G., et al. Two alternative conformations of a voltage-gated sodium channel. J. Mol. Biol. 425, 4074–4088 (2013). https://doi.org/10.1016/j.jmb.2013.06.036
[15] Irie, K., Shimomura, T., Fujiyoshi, Y. The C-terminal helical bundle of the tetrameric prokaryotic sodium channel accelerates the inactivation rate. Nat. Commun. 3, 793 (2012). https://doi.org/10.1038/ncomms1797
[16] Liao, M., Cao, E., Julius, D., Cheng, Y. Single particle electron cryo-microscopy of a mammalian ion channel. Curr. Opin. Struct. Biol. 27, 1–7 (2014). https://doi.org/10.1016/j.sbi.2014.02.005
[17] Matthies, D., Bae, C., Toombes, G. E., Fox, T., Bartesaghi, A., Subramaniam, S., et al. Single-particle cryo-EM structure of a voltage-activated potassium channel in lipid nanodiscs. eLife 7, e37558 (2018). https://doi.org/10.7554/elife.37558
[18] Tang, L., Gamal El-Din, T. M., Payandeh, J., Martinez, G. Q., Heard, T. M., Scheuer, T., et al. Structural basis for Ca^{2+} selectivity of a voltage-gated calcium channel. Nature 505, 56–61 (2014). https://doi.org/10.1038/nature12775
[19] Yue, L., Navarro, B., Ren, D., Ramos, A., Clapham, D. E. The cation selectivity filter of the bacterial sodium channel, NaChBac. J. Gen. Physiol. 120, 845-853 (2002). https://doi.org/10.1085/jgp.20028699
[20] Furini, S., Barbini, P., Domene, C. Effects of the protonation state of the EEEE motif of a bacterial Na^+-channel on conduction and pore structure. Biophys. J. 106, 2175–2183 (2014). https://doi.org/10.1016/j.bpj.2014.04.005
[21] Catterall, W. A. From ionic currents to molecular mechanisms: the structure and function of voltage-gated sodium channels. Neuron 26, 13–25 (2000). https://doi.org/10.1016/s0896-6273(00)81133-2
[22] Gur Barzilai, M., Reitzel, A. M., Kraus, J. E. M., Gordon, D., Technau, U., Gurevitz, M., et al. Convergent evolution of sodium ion selectivity in metazoan neuronal signaling. Cell Rep. 2, 242–248 (2012). https://doi.org/10.1016/j.celrep.2012.06.016
[23] Strong, M., Chandy, K. G., Gutman, G. A. Molecular evolution of voltage-sensitive ion channel genes: On the origins of electrical excitability. Mol. Biol. Evol. 10, 221–242 (1993). https://doi.org/10.1093/oxfordjournals.molbev.a039986
[24] Rahman, T., Cai, X., Brailoiu, G. C., Abood, M. E., Brailoiu, E., Patel, S. Two-pore channels provide insight into the evolution of voltage-gated Ca^{2+} and Na^+ channels. Sci. Signal. 7, ra109 (2014). https://doi.org/10.1126/scisignal.2005450
[25] Liebeskind, B. J., Hillis, D. M., Zakon, H. H. Independent acquisition of sodium selectivity in bacterial and animal sodium channels. Curr. Biol. 23, R948–R949 (2013). https://doi.org/10.1016/j.cub.2013.09.025
[26] Shimomura, T., Yonekawa, Y., Nagura, H., Tateyama, M., Fujiyoshi, Y., Irie, K. A native prokaryotic voltage-dependent calcium channel with a novel selectivity filter sequence. eLife 9, e52828 (2020). https://doi.org/10.7554/eLife.52828
[27] Hug, L. A., Baker, B. J., Anantharaman, K., Brown, C. T., Probst, A. J., Castelle, C. J., et al. A new view of the tree of life. Nat. Microbiol. 1, 16048 (2016). https://doi.org/10.1038/nmicrobiol.2016.48
[28] Irie, K., Haga, Y., Shimomura, T., Fujiyoshi, Y. Optimized expression and purification of NavAb provide the structural insight into the voltage dependence. FEBS Lett. 592, 274–283 (2018). https://doi.org/10.1002/1873-3468.12955

[29] Almers, W., McCleskey, E. W. Non-selective conductance in calcium channels of frog muscle: Calcium selectivity in a single-file pore. J. Physiol. 353, 585–608 (1984). https://doi.org/10.1113/jphysiol.1984.sp015352
[30] Wu, J., Yan, Z., Li, Z., Qian, X., Lu, S., Dong, M., et al. Structure of the voltage-gated calcium channel Cav1.1 at 3.6 Å resolution. Nature 537, 191–196 (2016). https://doi.org/10.1038/nature19321
[31] Mayer, M. L., Westbrook, G. L., Guthrie, P. B. Voltage-dependent block by Mg^{2+} of NMDA responses in spinal cord neurones. Nature 309, 261–263 (1984). https://doi.org/10.1038/309261a0
[32] Sobolevsky, A. I., Rosconi, M. P., Gouaux, E. X-ray structure, symmetry and mechanism of an AMPA-subtype glutamate receptor. Nature 462, 745–756 (2009). https://doi.org/10.1038/nature08624
[33] Lü, W., Du, J., Goehring, A., Gouaux, E. Cryo-EM structures of the triheteromeric NMDA receptor and its allosteric modulation. Science 355, aal3729 (2017). https://doi.org/10.1126/science.aal3729
[34] Fedele, L., Newcombe, J., Topf, M., Gibb, A., Harvey, R. J., Smart, T. G. Disease-associated missense mutations in GluN2B subunit alter NMDA receptor ligand binding and ion channel properties. Nat. Commun. 9, 957 (2018). https://doi.org/10.1038/s41467-018-02927-4
[35] Helliwell, K. E., Chrachri, A., Koester, J. A., Wharam, S., Verret, F., Taylor, A. R., et al. Alternative Mechanisms for Fast Na^{+}/ Ca^{2+} Signaling in Eukaryotes via a Novel Class of Single-Domain Voltage-Gated Channels. Curr. Biol. 29, 1503–1511 (2019). https://doi.org/10.1016/j.cub.2019.03.041
[36] Helliwell, K. E., Chrachri, A., Koester, J. A., Wharam, S., Taylor, A. R., Wheeler, G. L., et al. A novel single-domain Na^{+}-selective voltage-gated channel in photosynthetic eukaryotes. Plant Physiol. 184, 1674–1683 (2020). https://doi.org/10.1104/pp.20.00889
[37] Darszon, A., Nishigaki, T., Beltran, C., Treviño, C. L. Calcium Channels in the Development, Maturation, and Function of Spermatozoa. Physiol. Rev. 91, 1305–1355 (2011). https://doi.org/10.1152/physrev.00028.2010
[38] Stephens, R. F., Guan, W., Zhorov, B. S., Spafford, J. D. Selectivity filters and cysteine-rich extracellular loops in voltage-gated sodium, calcium, and NALCN channels. Front. Physiol. 6, 153 (2015). https://doi.org/10.3389/fphys.2015.00153